Supplementary Information

End-member decomposition

Following the approach of Gaillardet et al. (1999), we use a series of linear equations to solve for the proportions of sodium in the river that are attributed to evaporite, carbonate, and silicate weathering. Table 1 in the main text specifies the end-member molar ratios and their associated uncertainty. In order to propagate this uncertainty in end-member values through the calculation, we solve the linear equations for each river 10,000 times using a random sampling of weathering end-member values assuming a Gaussian distribution. For all of the calculations in the main text, the median and standard deviation of these Monte Carlo simulations were used as the solution and uncertainty for each river. For all rivers, using the median of the Monte Carlo simulations gives proportions attributed to each end-member that sum to 1 (± 0.05).

Although many of the rivers have distributions of Monte Carlo solutions that are roughly Gaussian for all three end-members (e.g. Supplementary Figure 1), there are a total of 12 of the 31 rivers whose solution distributions for either the evaporite or silicate (or both) end-members are not Gaussian and they have a long tail (e.g. Supplementary Figure 2). This is likely related to the fact that the end-member values for evaporites and silicates have overlapping ranges. In contrast the carbonate end-member values are more distinct resulting in Monte Carlo solution distributions for the carbonate end-member that are typically roughly Gaussian. These 12 rivers are: Brahmaputra, Fraser, Ganges, Kaoping, Kolyma, Lena, Maipo, Mekong, Orinoco, Red, Yangtze, and Yukon rivers.

We have tested the influence that these poorly constrained rivers with long tailed distributions have on the results from this study. If instead of using the medians of the distributions we use the modes for those rivers that do not have near Gaussian Monte Carlo distribution, the total fluxes reported in the main text change by <0.1 Tmol/y, well within the 0.2 Tmol/y uncertainty. However, it does make a slight difference for the proportions of sulfate attributed to each of the weathering end-members (and excess sulfate) for those 12 rivers. This difference influences where these rivers plot on Figure 6 (main text), and is illustrated in Supplementary Figure 3. Although these 12 rivers plot slightly differently in this figure, the major conclusion remains valid, namely that the rivers plot to the left of the 1:1 line and are farther from the line with increasing excess sulfate values, indicating that the excess sulfate likely has a low $\delta^{34}S$ value.

References

Gaillardet, J., Dupré, B., Louvat, P., Allegre, C.J., 1999. Global silicate weathering and CO2 consumption rates deduced from the chemistry of large rivers. Chemical Geology 159, 3–30.

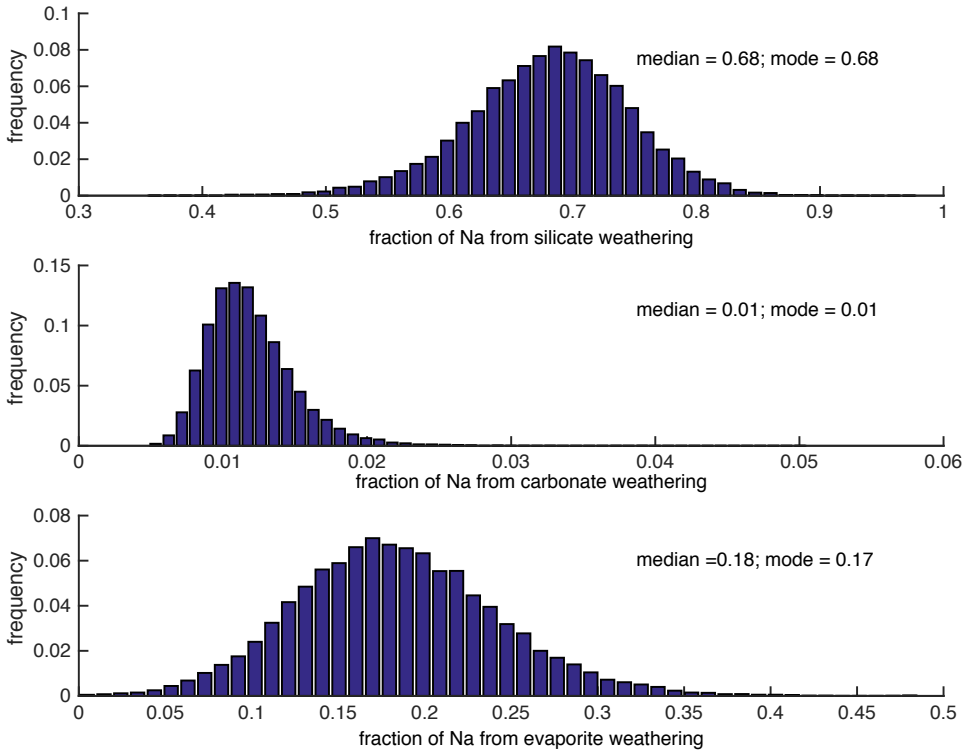

Supplementary Figure 1. Example of Monte Carlo solution distributions for the proportion of Na derived from silicate (top), carbonate (middle), and evaporite (bottom) for the Meghna river. This illustrates the Gaussian nature of the three end-member distributions. N.B. the x-axis is scaled differently for the three plots.

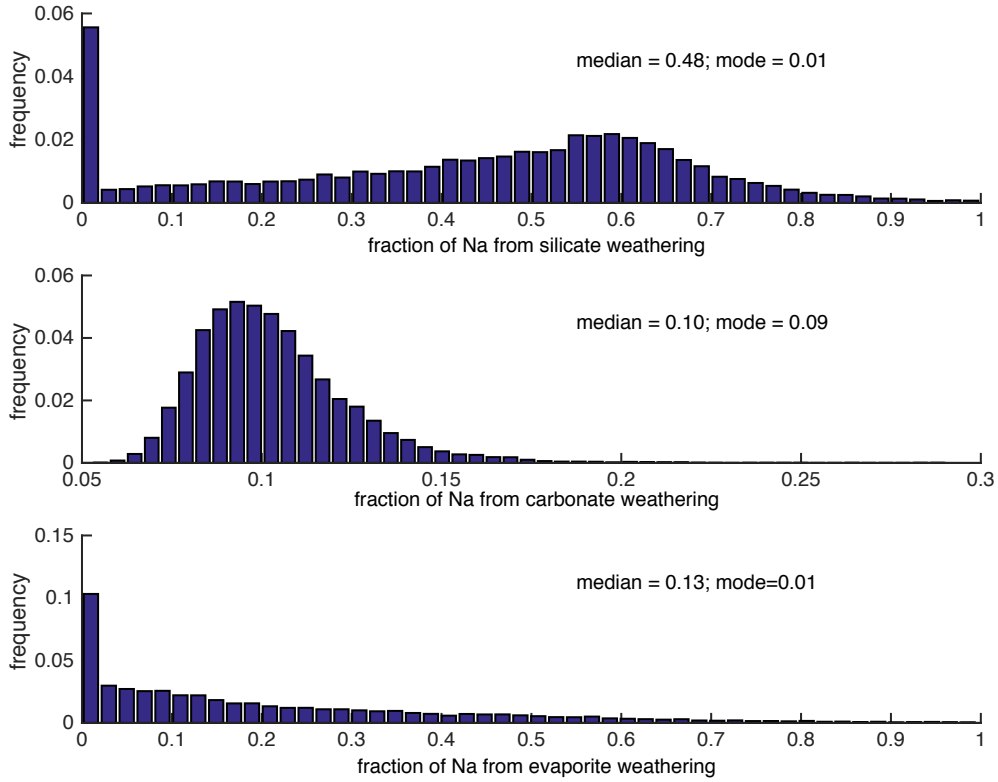

Supplementary Figure 2. Example of Monte Carlo solution distributions for the proportion of Na derived from silicate (top), carbonate (middle), and evaporite (bottom) for the Yukon river. Note that both the silicate and evaporite distributions are highly skewed and have a mode near zero.

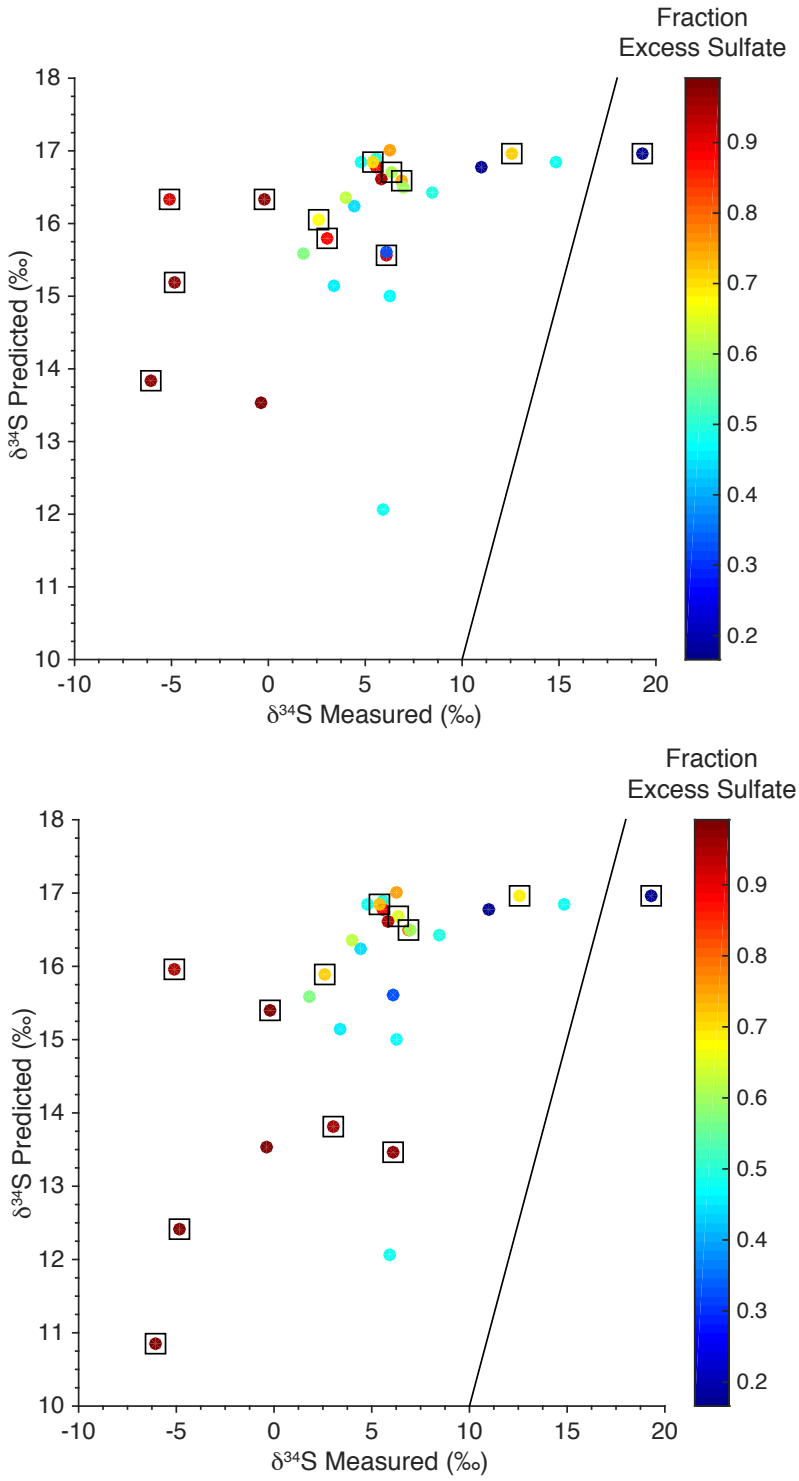

Supplementary Figure 3. (top) same as Figure 6 (main text) with the 12 non-Gaussian rivers indicated by squares around the marker. (bottom) same as Figure 6 (main text) but using the mode of the Monte Carlo distribution instead of the median for the 12 non-Gaussian rivers indicated by the black squares.